Cement and Concrete Composites 74 (2016) 7–15

Contents lists available at ScienceDirect

Cement and Concrete Composites

journal homepage: www.elsevier.com/locate/cemconcomp

The effect of accelerated aging on the interface of jute textile reinforced concrete

Maria Ernestina Alves Fidelis [a], Romildo Dias Toledo Filho [a, *], Flávio de Andrade Silva [b], Viktor Mechtcherine [c], Marko Butler [c], Simone Hempel [c]

[a] Department of Civil Engineering, COPPE, Universidade Federal do Rio de Janeiro, P.O. Box 68506, CEP 21941-972, Rio de Janeiro, RJ, Brazil
[b] Department of Civil Engineering, Pontifícia Universidade Católica do Rio de Janeiro (PUC-Rio), Rua Marques de São Vicente 225, 22451-900, Rio de Janeiro, RJ, Brazil
[c] TU Dresden, Institute of Construction Materials, 01062, Dresden, Germany

ARTICLE INFO

Article history:
Received 20 January 2016
Received in revised form
12 August 2016
Accepted 3 September 2016
Available online 6 September 2016

Keywords:
Durability
Accelerated aging
Textile reinforced concrete
Mechanical test
Jute fiber

ABSTRACT

In this work the degradation mechanisms of concrete reinforced with natural jute textile are discussed. Double-sided pullout tests were performed on specimens reinforced with polymer-coated and uncoated jute fabrics. To obtain a composite with an enhanced durability performance a matrix with partial replacement of the Portland cement by metakaolin was used. Before testing, the specimens were subjected to accelerated aging conditions. After a curing period of 28 days in water the samples were exposed to a temperature of 40 °C and a relative humidity of 99% over 28, 56, 90, 180 and 365 days. Microstructural analyses were performed to evaluate the degradation of the jute yarn and the fiber-matrix interphase using an environmental scanning electron microscope. Thermogravimetric analysis was carried out in order to evaluate the calcium hydroxide content. The pullout results showed that coated fabrics formed a stronger bond than did the uncoated. For ordinary Portland cement matrix the maximum fiber pullout force decreased up to 85% after six months of accelerated aging. In the MK matrix the degradation process was retarded substantially. Polymer coatings improved the bond between fiber and matrix and reduced fiber degradation.

1. Introduction

Natural fibers have been widely studied as a means of reinforcement in cementitious matrices [1–4]. In an alkaline environment fiber degradation occurs, and much has been discussed about how to improve the durability of composites with natural fibers [3–16]. As a result, modifications to the matrices, such as the partial replacement of Portland cement by pozzolanic material, have been tried in order to obtain a matrix with a low calcium hydroxide content [3,4,17,18]. The degradation of natural fiber reinforced composites can also be attributed to the damage occurring to the fiber-matrix interface due to changes in the fibers' volumes within the matrix [7,18–20].

In addition to modifications in the matrix, fiber treatments are often performed in order to remove extractives and wax on the fiber surface, to improve the volumetric stability of the fiber and to enhance the fiber-matrix stress transfer [21–27]. Scheffler et al. [24] observed improvements in the mechanical performance of composites reinforced with glass fibers impregnated with styrene butadiene by increasing the resistance to the alkaline environment in the matrix. Mäder et al. [25] reported a strengthening of the fiber-matrix bond in composites with glass and carbon fibers impregnated with styrene butadiene.

Ferreira et al. [26,27] reported that the hornification treatment promotes an enhancement in the fiber-matrix bond due to the modifications in the fiber structure. This improvement is related to the treated fibers' lower water absorption capacity, demonstrated using absorption testing and microstructural analysis. The authors also investigated the influence of controlled alkaline treatment (calcium hydroxide solution) in the fiber-matrix bonding. The results showed that this treatment improved the bond strength once waxes, fats and other amorphous constituents of the fiber were partially removed, increasing the fiber crystallinity and superficial roughness.

In the case of textile-reinforced concrete, the bond behavior is

* Corresponding author.
E-mail address: toledo@coc.ufrj.br (R.D. Toledo Filho).

http://dx.doi.org/10.1016/j.cemconcomp.2016.09.002
0958-9465/

completely different from other materials used as reinforcement since the cross section of the fabric is not homogeneous. Fabrics are composed of yarns, which are in turn composed of filaments. The external filaments of a yarn have direct contact with the matrix; in other words, only a part of the fabric is anchored in the matrix. The internal filaments are not affected by the hydration products of the cement. Thus, there is only friction between the filaments. When the reinforcement is subjected to treatment with polymer, a complete anchoring of all filaments takes place, making the bond between the filaments stronger than the adhesion of the fiber with the matrix [28].

Mumenya et al. [29] investigated the fiber-matrix interface of textile-reinforced concrete using a polypropylene hybrid fiber. The investigation was performed using pullout tests after accelerated aging conditions consisting of 100 cycles of wetting and drying. The results showed no major changes in respect of toughness. There was a small reduction in the peak load values after the wetting and drying cycles due to the following mechanisms: during the wetting cycle there was an increase in the hydration reactions, resulting in a strengthening of the fiber-matrix bond, while the drying cycle induced the formation of microcracks, resulting in a reduction of the peak load value.

Butler et al. [30] investigated the bond to multi-filament yarns of AR-glass through pullout tests performed on samples subjected to accelerated aging. They also studied the influence of matrix composition and observed that the use of pozzolans such as metakaolin and fly ash provided promising results. The maximum fiber pullout force decreased by only approximately 25% after one year of accelerated aging while the work to fracture W0.25 and W0.5 decreased by approximately 40% in comparison to the reference. The eventual tests on TRC specimens confirmed that an appropriate matrix composition with reduced OPC content and addition of pozzolana is a prerequisite for favorable interface microstructure and, hence, favorable properties in TRC reinforced with glass fiber [31]. In this case the tensile strength and strain capacity of TRC can be preserved without dramatic losses over decades of exposure to ordinary climate. For matrix compositions with high OPC content, may result at a TRC age of as early as few months or years in a dramatic decrease of the mechanical performance and changes in the failure behavior of the composite from quasi-ductile to brittle. The essential cause of such losses was discovered to be the microscopic densification of the fiber-to-matrix interface. This led to increased bond intensity and restricted slip-ability of the filaments [32].

The durability of the interface of cementitious composites reinforced with AR-glass was analyzed by Bentur et al. [33]. The AR-glass fabric was impregnated with different slurries, such as microsilica nano-particles and polystyrene and styrene acrylic polymers. Pullout tests were carried out before and after several accelerated aging regimes. It was observed that for the treatment with microsilica, the nano-particles were retained within the yarn, while the polymers formed a thin film over the fibers. Regarding durability the best results were observed for those fibers treated with microsilica nano-particles. The specimens treated with microsilica had higher initial load and energy levels after aging, exhibiting excellent properties as compared to the reference. The energy values for aged polymer systems were 50% higher than the reference, while for microsilica systems, they were 100% higher.

In contrast to the interest in man-made fibers, there is a scarcity of studies about the durability of the interface of vegetable fibre textile-cementitious composites. The existing results are mainly related with the nature of the transition zone of individual vegetable fibers and cellulose pulps with cement matrices [8,9,34,35]. There are also studies about the pullout behavior of single vegetable fibers from cement matrices [26,27,36] and about the durability of vegetable fiber cementitious composites exposed to different external environments [3–7,10–16,37].

This research aims, therefore, to fill the gap existing in the literature investigating the bonding behavior, before and after aging, of textile cementitious composites using a jute fabric as reinforcement. A matrix with a low calcium hydroxide content was developed. In addition to the matrix modification, fiber treatment with a polymer was performed in order to improve the volumetric stability of the fiber, the fiber-matrix stress transfer, and the durability of the composites. Double-sided pullout tests were performed on both aged and non-aged specimens. Micro-structural analysis using an environmental scanning electron microscope was carried out to evaluate the degradation of the jute fiber and of its interface with the cement based matrix. Thermogravimetric analysis was performed in the cementitious matrices in order to verify the consumption of calcium hydroxide in the MK matrix and to explain the fiber degradation mechanisms after the aging process.

2. Materials and processing

2.1. Jute fibers

Jute is commercially available as a long strand, from which the fabrics are produced. It is extracted from the stem of the plant *Corchorus capsularis* by a combination of processes comprised of the following steps: cutting, retting, shredding, drying, packing, and classification. Uncoated yarn has a mass of 326 tex and coated yarn 639 tex. Styrene-butadiene polymer was used to impregnate the fibers. The polymer forms a film protecting the fiber, thus preventing contact of the fiber with the hydration products. This polymer is commonly used in impregnating glass and carbon fibers [24,38]. The fibers were impregnated in the laboratory for 10 min. Table 1 presents the properties of coated and uncoated jute yarn.

2.2. Matrix and specimen preparation

The matrix was produced using Portland cement CPII F-32 defined by the Brazilian standard [39] as composed of filler (in mass: 85% < clinker < 91%; 3% < gypsum < 5%; 6% < filler < 10%) with a 28 days compressive strength of 32 MPa; metakaolin obtained from Metacaulim do Brasil, coarse sand with maximum diameter of 1 mm, a naphthalene superplasticizer, and styrene-butadiene polymer for fiber impregnation with a content of 30% solids. Table 2 summarizes the matrix composition. In the present work the abbreviations “OPC matrix” and “MK matrix” were used for matrix with only cement as a binder and matrix with cement replacement by metakaolin, respectively.

The mortar matrices used in this study were designed of two mixes: 1:1.2:0.44 (OPC: sand: water-to-cement ratio) and 1:1.2:0.48 (0.5 OPC: 0.5 metakaolin: sand: water-to-cement ratio) with 12 kg/m^3 of superplasticizer.

The pullout specimens were produced in the form of thin plates

Table 1
Physical and mechanical properties of the yarn.

Properties	Uncoated	Coated
Fineness [tex[a]]	326	639
Diameter [mm]	0.785	0.804
Number or filaments	141	141
Tensile strength [MPa]	104	88
Strain-to-failure [%]	2.11	2.28
Young's modulus [GPa]	5.68	4.46

[a] Mass in g of 1 km yarn (tex = g/km).

Table 2
Matrix composition.

Mix ingredients	OPC matrix	MK matrix
	[kg/m^3]	
Cement CPII F-32	835	399
Metakaolin	–	399
Sand 0/1	1002	957
Water	365	372
Superplastisizer	–	12

with variable thicknesses (5 mm in the middle and 10 mm in the ends) with a width of 50 mm, as shown in Fig. 1. A notch depth of 1 mm was used.

The specimens were reinforced with a single layer of jute fabric. The reinforcement was placed over the mold before pouring the mortar matrix in order to allow the correct impregnation of the matrix. The specimens were demolded one day after fabrication. Then they were stored up to an age of 28 days in water at 20 °C. After that the samples were subjected to accelerated aging at a temperature of 40 °C and 99% relative humidity. Reference specimens were stored in a controlled laboratory environment at 20 °C and 65% relative humidity. The samples subjected to accelerated aging were removed from the aging process 3 days prior to testing and stored under conditions of 20 °C and 65% relative humidity until testing. Steel plates were glued on the ends of the specimens and fixed between the clamping jaws of the testing machine.

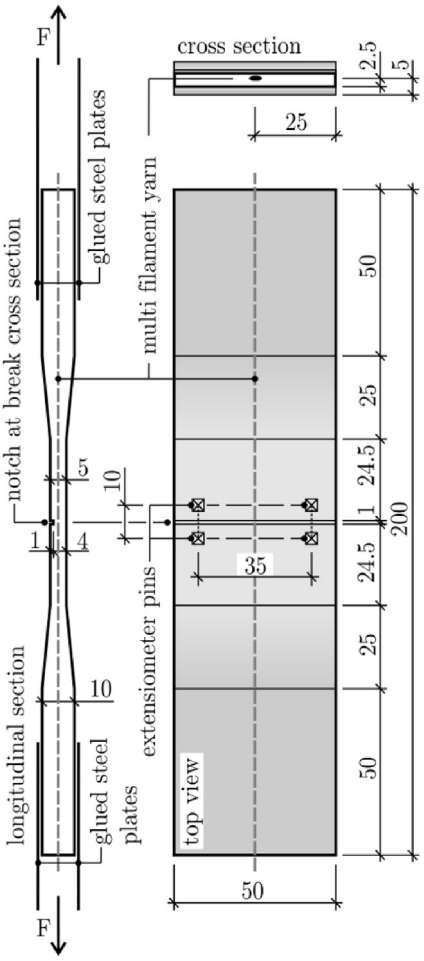

Fig. 1. Dimensions of specimen and arrangements of load adapters and crack width sensors for double-sided pullout test.

3. Experimental testing procedure

The pullout tests were performed in a servo-hydraulic universal testing machine under a displacement-control regime. The initial displacement rate was 0.5 mm/min until the matrix cracked at the notched section. Thereafter the displacement rate was altered to 1 mm/min until the crack opening reached 4 mm or until failure of the specimen. The test results, such as the values of load, crack width, and displacement of the crosshead of the testing machine were measured and recorded. Precision gauges were fixed in the vicinity of the crack in order to measure the crack opening with accuracy. Fig. 2 shows the test arrangement.

After testing the fiber and fiber-matrix-interface were investigated using an environmental scanning electron microscope (ESEM) model XL30 (FEI Philips Company, Netherlands). The ESEM was operated under a low vacuum. All the micrographs were taken under the gaseous secondary electron (GSE) detector mode at accelerating voltages of 20 and 30 kV and chamber pressure of 0.6–0.7 mBar. No coating with carbon or gold, as is customary for a high-vacuum SEM, was required.

Thermal analysis was performed for OPC and MK matrices at 28 and 180 days. The tests were performed in a SDT Q600 simultaneous TGA/DTA/DSC from TA Instruments. The equipment was operated at a heating rate of 10 °C/min from room temperature to 1000 °C, in a platinum crucible in nitrogen atmosphere with flow of 100 ml/min. The samples were firstly dried at 35 °C for 1 h within the equipment.

4. Results and discussion

Fig. 3 shows the schematic representation of a complete load vs. crack opening curve as measured in the double-sided pullout test. The curve was divided into three zones according to the theoretical background presented in Ref. [30]. Zone I represents the behavior of uncracked specimens up to matrix cracking, i. e., until appearance

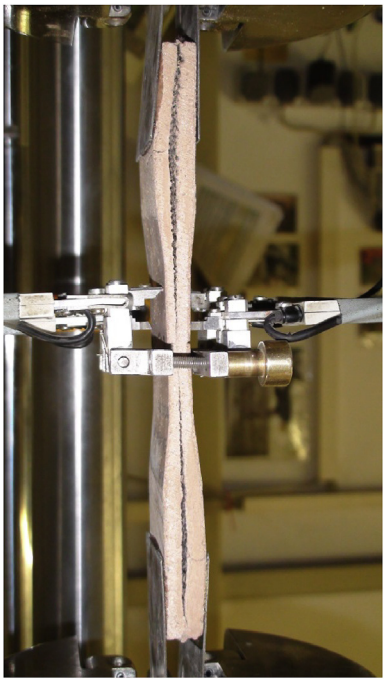

Fig. 2. Clamped pullout specimen instrumented with extensometers.

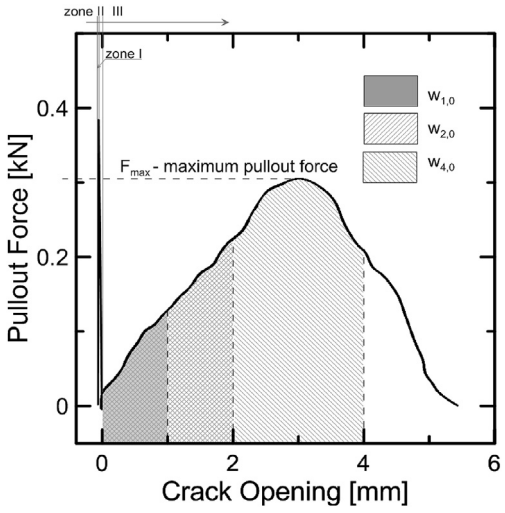

Fig. 3. Schematic view of a typical pullout curve. Adapted from Ref. [30].

of the first crack. Zone II corresponds to the sudden drop in load happening because the fiber content is less than the critical amount and, therefore, is not enough to withstand the load imposed. When the fiber-matrix bond is very pronounced, the specimen fails in Zone II. Finally, in Zone III typical multifilament yarn pullout is represented. In this phase the single filaments are stretched in different manners during crack opening, due to the fiber/matrix bond characteristics. After the maximum pullout load, Fmax, is reached, complete failure of the filaments occurs, characterized by a softening behavior in the matrix.

In Fig. 4 pullout force vs. crack opening curves are presented for uncoated and coated fabrics in the OPC matrix. Fig. 5 shows the curves for the MK matrix. The curves were plotted in Zone III only in order to simplify the graphic representation. In those cases where it was impossible to distinguish Zone II from Zone III due to the continuous drop in the curve, the graph was plotted to include Zone II. Each curve was selected from a collection of up to 10 individual curves representing the typical behavior.

Four parameters were defined to facilitate comparison among the results. They were maximum force (F_{max}), work to fiber pullout, W1.0, W2.0 and W4.0, corresponding to crack openings of 1.0, 2.0 and 4.0 mm, respectively and WF_{max}, corresponding to the crack opening of Fmax. The calculation of these parameters was made for each measured curve, which allowed visualization of the scatter of the results, as shown in Tables 3 and 4 and in Figs. 6 and 7, for OPC matrix and MK matrix, respectively. Figs. 6 and 7 show the maximum pullout force for each individual sample following the accelerated aging regimes (28, 56, 90, 180 and 365 days), as well as the pullout values of work to crack openings of 1.0, 2.0 and 4.0 mm were indicated for each different aging period. In addition, Tables 3 and 4 give the average values and the associated standard deviations.

Examination of the results in Table 4 (MK matrix) points out that the maximum load values for coated fabrics were higher than those for the uncoated fabrics. The same was true for the OPC matrix (Table 3), although in this case the specimens with coated fibers did not stand up to the aging time of 365 days. For uncoated fabrics (OPC matrix) after up to 90 days of aging, there are no significant differences in maximum pullout force, but there was a decrease in the energy absorption capacity. For 180 and 365 days of aging, the pullout load values and work capacity were similar. However, for coated yarns (OPC matrix), there were no large differences in the bond and work to pullout values (up to 90 days). At 180 days of accelerated aging, failure of the specimens occurred.

For the uncoated fabrics (MK matrix), the load values and work to pullout were similar, for all aging times. In the case of the coated fabric (MK matrix), there was a small decrease in the force, whereas the work to pullout values were similar. Comparing the matrices, the tests results of MK matrix were better due to the pozzolanic reactions, as can be observed through thermogravimetric analysis carried out in the OPC and MK matrices at 28 and 180 days (see Fig. 8 and Table 5). In addition the coating film possibly protects the fiber, avoiding contact with the hydration products. The percentage of total combined water and $Ca(OH)_2$ content was calculated in relation to calcined mass of cement [40,41]. It can be observed that for the MK system the total amount of combined water was higher than for the OPC matrix. Also, note that the very small amount of CH observed in the MK matrix after 28 days (smaller than 0.5%) of cure and it was totally consumed after 180 days of age.

It can be seen in Figs. 4 and 5, that for both matrices the polymer increases the interface stiffness. This is demonstrated by the WF_{max} values (Tables 3 and 4), which are lower for the specimens with treated fibers (except for reference, OPC matrix and 28d, MK matrix). It is a very positive feature, since it means that the yarn is activated at smaller crack openings and thus it limits crack openings effectively.

Through the study of fiber-matrix interface it can be observed

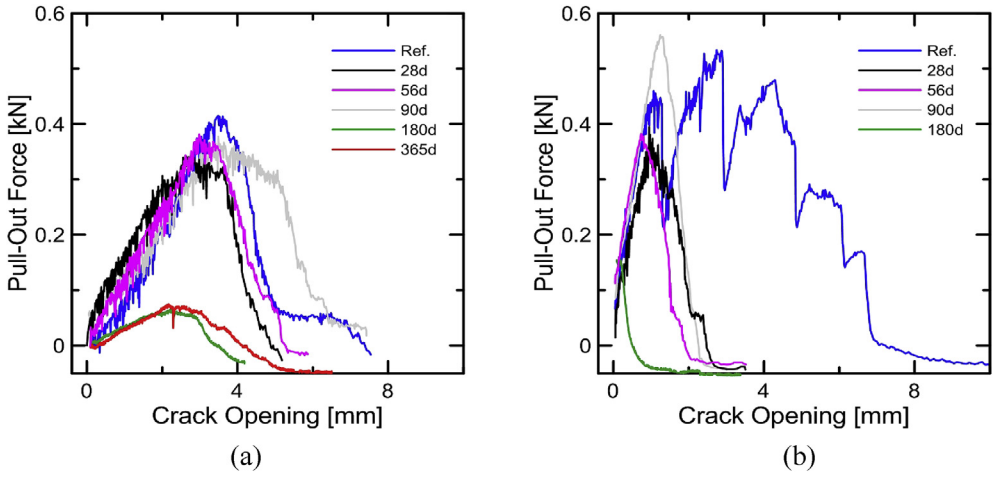

Fig. 4. Influence of aging time on the pullout resistance of jute textile from an OPC matrix: (a) uncoated and (b) coated fibers; selected, representative curves are shown.

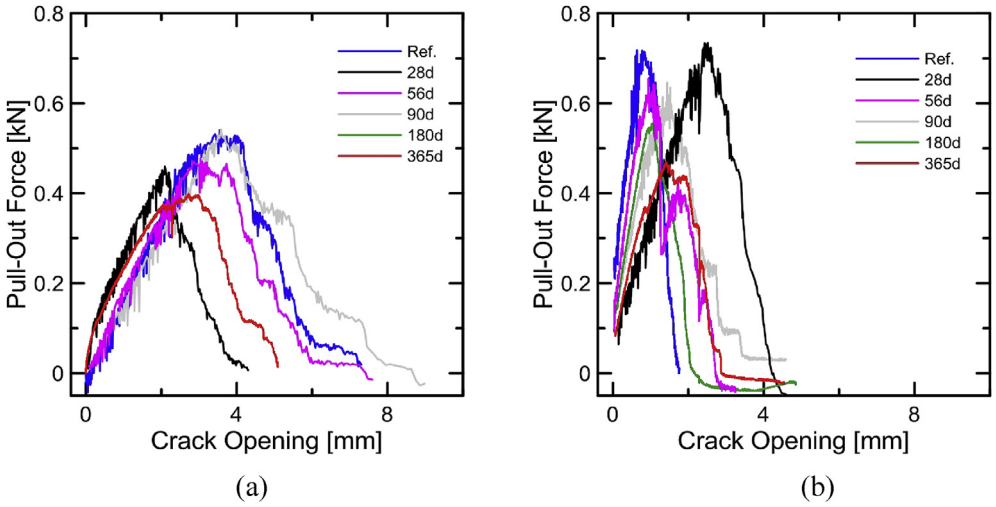

Fig. 5. Influence of aging time on the pullout resistance of jute textile from a cementitious MK matrix: (a) uncoated and (b) coated fibers; selected, representative curves are shown.

Table 3
Summary of pullout test results performed on coated and uncoated jute fibers (mean values); standard deviations in parentheses – OPC matrix.

Aging time (days)	Uncoated fibers					Coated fibers				
	F_{max} [kN]	$W_{Fmax\ [J]}$	$W_{1.0}$ [J]	$W_{2.0}$ [J]	$W_{4.0}$ [J]	F_{max} [kN]	$W_{Fmax\ [J]}$	$W_{1.0}$ [J]	$W_{2.0}$ [J]	$W_{4.0}$ [J]
Ref.	0.48 (0.08)	0.94 (0.30)	0.08 (0.03)	0.28 (0.06)	1.06 (0.18)	0.52 (0.05)	0.95 (0.89)	0.27 (0.04)	0.62 (0.06)	1.09 (0.34)
28 d	0.36 (0.06)	0.53 (0.09)	0.10 (0.01)	0.31 (0.03)	0.87 (0.09)	0.45 (0.08)	0.41 (0.20)	0.21 (0.08)	0.47 (0.10)	0.76 (0.21)
56 d	0.36 (0.04)	0.55 (0.14)	0.05 (0.03)	0.21 (0.07)	0.75 (0.12)	0.47 (0.03)	0.27 (0.07)	0.30 (0.04)	0.49 (0.05)	–
90 d	0.32 (0.11)	0.68 (0.18)	0.04 (0.03)	0.16 (0.10)	0.52 (0.27)	0.64 (0.10)	0.60 (0.22)	0.36 (0.09)	0.79 (0.15)	–
180 d	0.07 (0.02)	0.05 (0.03)	0.03 (0.02)	0.06 (0.05)	0.13 (0.07)	0.17 (0.03)	0.02 (0.02)	–	–	–
365 d	0.06 (0.03)	0.06 (0.03)	0.01 (0.01)	0.06 (0.03)	0.14 (0.02)	–	–	–	–	–

Table 4
Summary of pullout test results performed on coated and uncoated jute fibers (mean values); standard deviations in parentheses – MK matrix.

Aging time (days)	Uncoated fibers					Coated fibers				
	F_{max} [kN]	$W_{Fmax\ [J]}$	$W_{1.0}$ [J]	$W_{2.0}$ [J]	$W_{4.0}$ [J]	F_{max} [kN]	$W_{Fmax\ [J]}$	$W_{1.0}$ [J]	$W_{2.0}$ [J]	$W_{4.0}$ [J]
Ref.	0.57 (0.06)	1.68 (0.78)	0.10 (0.03)	0.36 (0.10)	1.18 (0.25)	0.75 (0.06)	0.46 (0.19)	0.48 (0.05)	0.97 (0.10)	–
28 d	0.48 (0.10)	0.68 (0.25)	0.17 (0.04)	0.53 (0.09)	1.12 (0.38)	0.66 (0.11)	1.05 (0.69)	0.27 (0.07)	0.71 (0.10)	1.61 (0.17)
56 d	0.49 (0.09)	1.15 (0.30)	0.09 (0.04)	0.33 (0.10)	1.12 (0.30)	0.59 (0.05)	0.63 (0.20)	0.31 (0.08)	0.73 (0.08)	1.13 (0.26)
90 d	0.46 (0.10)	1.36 (0.36)	0.05 (0.04)	0.21 (0.14)	0.73 (0.43)	0.61 (0.05)	0.67 (0.31)	0.30 (0.05)	0.73 (0.09)	1.43 (0.27)
180 d	0.52 (0.07)	1.55 (0.36)	0.05 (0.03)	0.21 (0.11)	0.89 (0.21)	0.57 (0.08)	0.59 (0.26)	0.34 (0.06)	0.76 (0.09)	1.47 (0.22)
365 d	0.40 (0.04)	0.71 (0.09)	0.11 (0.08)	0.34 (0.20)	0.92 (0.20)	0.53 (0.07)	0.45 (0.15)	0.33 (0.05)	0.69 (0.12)	0.85 (0.38)

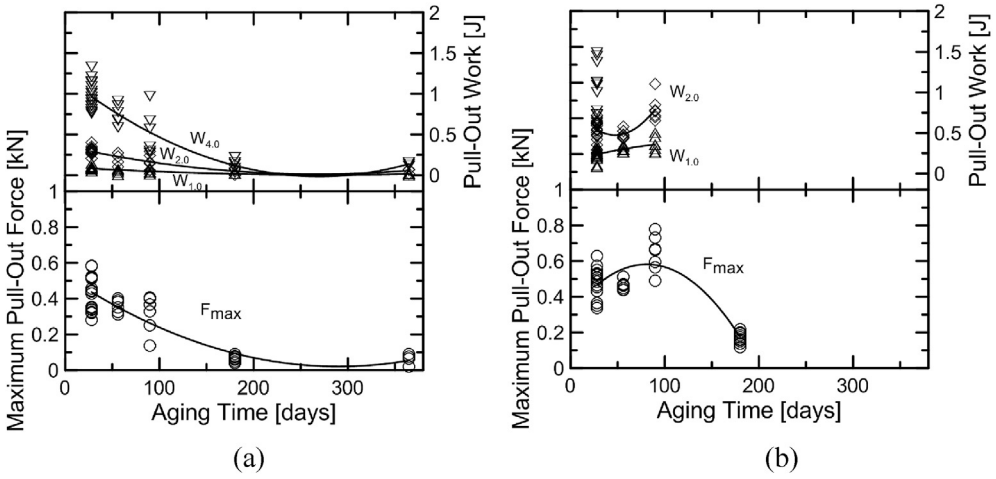

Fig. 6. Influence of aging time on the maximum pullout force and on the work to pullout of (a) uncoated and (b) coated jute yarns in an OPC matrix.

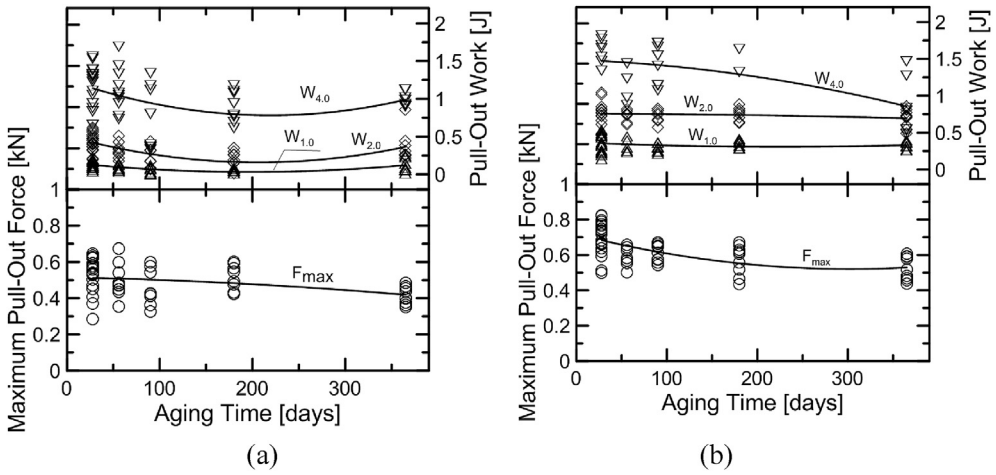

Fig. 7. Influence of aging time on the maximum pullout force and on the work to pullout of (a) uncoated and (b) coated jute yarns, on a MK matrix.

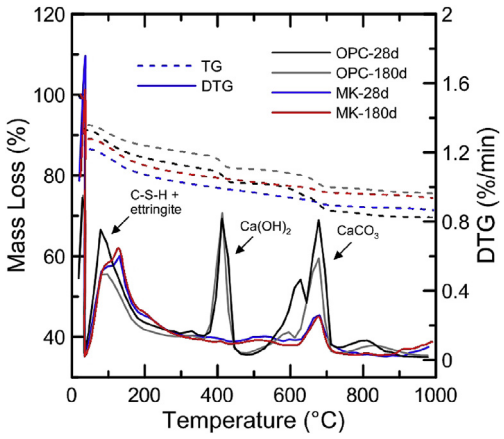

Fig. 8. TG and DTG analysis performed in PC and MK matrices at 28 and 180 days.

Table 5
Percentage of total combined water and calcium hydroxide in the cement calcined basis.

Matrix	Age (days)	Total combined water (%)	$Ca(OH)_2$ (%)
OPC	28	16.11	14.42
	180	11.78	13.17
MK	28	21.60	0.49
	180	20.24	0.00

that in addition to reducing the alkalinity of the matrix due to the pozzolanic reactions, hydration products fill the pores of the matrix and the interphase, reducing the total porosity of the composite and resulting in improved mechanical behavior and probably reducing deterioration of the fibers.

The coating was responsible for improving the bond, except at 365 days in the aging process (OPC composites). According to Yang et al. [42] and Chakraborty et al. [43], a portion of the carboxylic acids of the styrene butadiene copolymer reacts with calcium hydroxide, forming water as a byproduct. One hypothesis is that in the OPC matrix, the free pore water can dissolve the calcium hydroxide, thus facilitating the absorption of calcium ions by the polymer. This may have been responsible for the loss of integrity in the coating. This is a different process than the one occurring in the MK system, where the pozzolanic reactions consumed the calcium hydroxide protecting the polymer and fiber from degradation.

Generally, the coating protects the fiber from the hydration products; it reduces the water absorption of the fiber, enhancing its volumetric stability and consequently reducing the variation of the pores in the interface. The coating, coupled with the use of pozzolans, contributed to increase the fiber-matrix bond as well as the fiber durability, since the polymer forms a film protecting the fiber, while the pozzolanic reactions make the matrix denser, also protecting the coating from reaction with $Ca(OH)_2$.

Figs. 6 and 7 provide the values of the parameters derived from individual measurements and give the corresponding non-linear regression curves for OPC and MK matrices. The maximum fiber pullout force (F_{max}) decreased by approximately 85% and 67% for uncoated and coated fibers in the OPC matrix, respectively, after six months of accelerated aging. F_{max} decreased by approximately 9% and 24% for uncoated and coated fiber in the MK matrix, respectively, after six months of accelerated aging.

Fig. 9 shows stereo-light microscope images of the fiber surface and typical morphology of the interface zone between multifilament yarns in the OPC matrix. For uncoated fibers, the matrix does not seem well incorporated into the fibers in the OPC matrix (Fig. 9a), while for coated yarn it can be seen that due to the impregnation, the jute fiber textile is better incorporated into the matrix (Fig. 9b).

Fig. 10 shows micrographs of uncoated and coated fabrics in the MK matrix. It is observed that the fibers seem not to be so loose as the fibers in the OPC matrix, possibly due to the absence of an alkali attack and the mineralization of the fibers (Fig. 10a). Regarding the coated yarn, due to the impregnation there is more intense contact between the fibers and the matrix, but not as strong as between the jute in the OPC matrix (Fig. 10b).

Figs. 11 and 12 show micrographs of the fiber at the interfacial zone. For uncoated fibers in the OPC matrix, it can be seen that Portlandite crystals have grown between the brittle jute fibers at the interface (Fig. 11a), while for coated yarn the fibers are protected against the alkali by the impregnation, but they break because the bond is very strong and the fibers cannot freely deform (lack of free length). The images are from specimens submitted to 365 days of accelerated aging. In a previous work [32], this microstructural phenomenon was described and related to the mesoscopic material behavior of TRC reinforced with AR-glass fiber by means of a phenomenological bond model.

In Fig. 12 micrographs of uncoated and coated yarns in the MK matrix are presented. It was observed that the hydration products

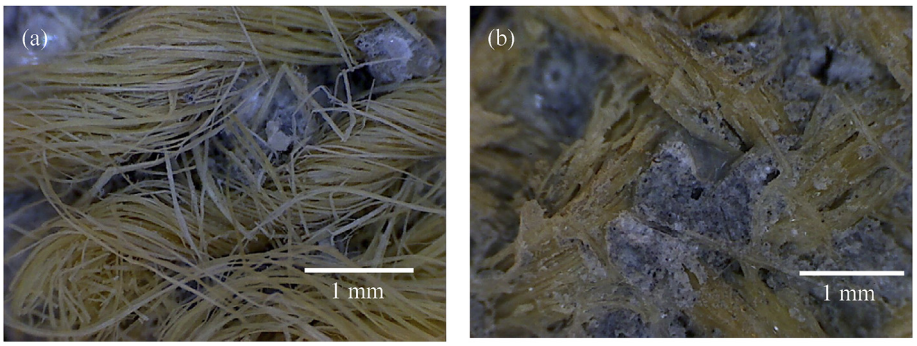

Fig. 9. Images from stereo-light microscope for OPC Matrix samples: (a) Uncoated fiber and (b) Coated fiber.

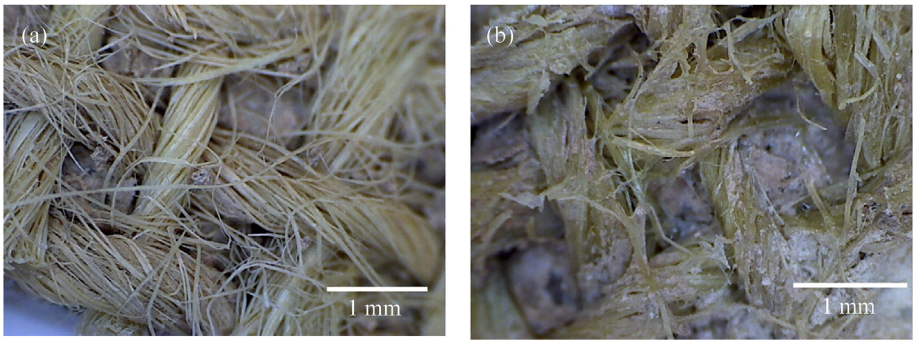

Fig. 10. Images from a stereo-light microscope for MK matrix samples: (a) Uncoated fiber and (b) Coated fiber.

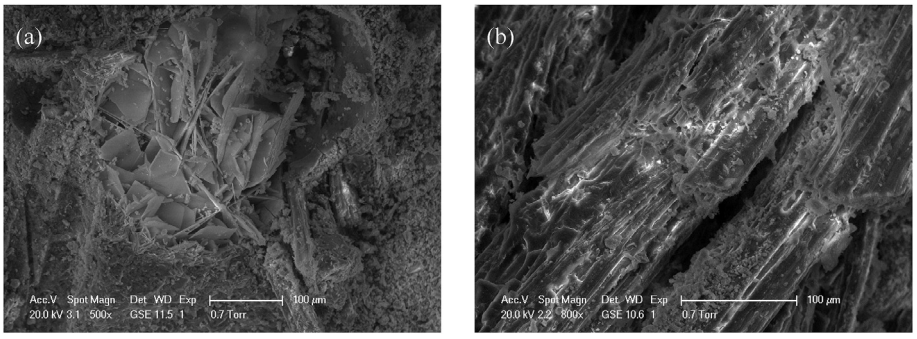

Fig. 11. Jute-fiber-matrix interface in an OPC matrix after 365 days of accelerated aging: (a) Uncoated fiber (b) Coated fiber.

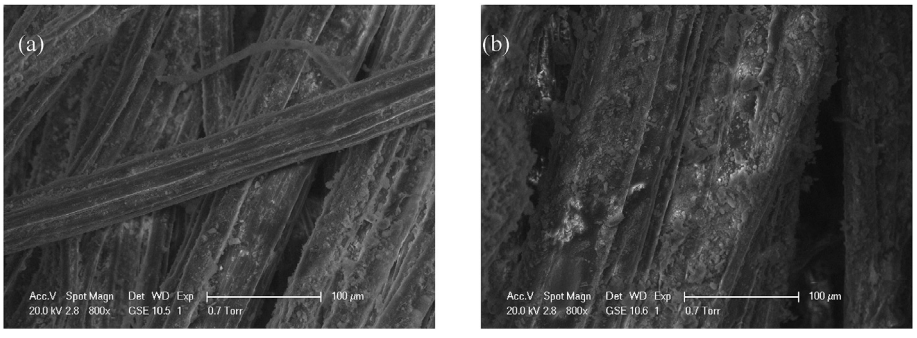

Fig. 12. Jute-fiber-matrix interface in a MK Matrix after 365 days of accelerated aging: (a) Uncoated fiber (b) Coated fiber.

had grown on the surface of the yarns but the fiber itself was not attacked. No Portlandite was found in the matrix (Fig. 12a). For coated yarns it can be seen that the fibers are covered with a thick layer of polymeric material. The polymer impregnated yarns seem

to be in good condition and the hydration products are grown together with the impregnation layer, even after 365 days of accelerated aging (Fig. 12b).

Evaluating the results, it can be seen that changes in the fiber-matrix interface can modify the mechanical behavior of the composite, influencing the strength and pullout work. The essential cause of the low-performance observed for the OPC matrix composites is related to the high alkalinity in the pores of the matrix. The composites with metakaolin yielded superior results since their stable interface could be observed for the entire aging interval, except at 365 days.

5. Conclusions

The following conclusions can be drawn from the present work on the interface properties of jute-textile-reinforced concrete exposed to accelerated aging:

- Double-sided pullout tests performed after accelerated aging showed that the OPC composite system yielded better results for specimens with coated fabric, although at 180 days there was a complete loss of ductility. At 180 days of aging, the matrix and coated fibers showed major signs of degradation, and no typical fiber pullout could be observed due to the failure of the fabric immediately after the cracking of the matrix. At 365 days of aging the specimens could no longer withstand the aging process. The hypothesis is that the aging process became more severe at 365 days for OPC matrix – coated fabric, since a reaction may have occurred between the coating and calcium hydroxide, while in the matrix with metakaolin the pozzolanic reactions consume the calcium hydroxide, leading to an increase in the density of the matrix and thus protecting the fiber and coating.
- For the MK composites the mechanical performance was only slightly affected by the accelerated aging. Even after 365 days of aging the specimens yielded high values of maximum force and work to pullout. The impregnation process was effective, providing better performance in the MK matrix. The coating together with the pozzolan produced the best bonding properties between fabric and matrix. The pozzolan in the metakaolin consumed the calcium hydroxide, reducing alkalinity in the pore solution, hence avoiding the fiber degradation. Moreover, the metakaolin was also beneficial in protecting the polymer.
- It was observed an increase in the interface stiffness due to the coating. Such behavior is considered beneficial since if the coated yarn is activated at a smaller strain this may limit the crack opening.
- Microstructural observation suggested that the jute fibers undergo a mineralization process when used as reinforcement in conventional Portland cement matrix. It was possible to observe Portlandite crystals between the fibers and the interface. No signs of fiber degradation were noticed for jute fibers exposed to the aging process in the MK composites. No Portlandite was observed in micrographs of the MK matrix, and the polymer coated fibers seem to be in good condition. Thermal analysis was performed and confirmed the consumption of calcium hydroxide in the MK matrix.

References

[1] R. Jarabo, E. Fuente, M.C. Monte, H. Savastano Jr., P. Mutjé, C. Negro, Use of cellulose fibers from hemp core in fiber-cement production. Effect on flocculation, retention, drainage and product properties, Ind. Crops Prod. 39 (2012) 89–96.
[2] M.G. Sierra Beltran, H.M. Jonkers, E. Schlangen, Characterization of sustainable bio-based mortar for concrete repair, Constr. Build. Mater. 67 (C) (2014) 344–352.
[3] R.D. Toledo Filho, F.A. Silva, E.M.R. Fairbairn, J.A. Melo Filho, Durability of compression molded sisal fiber reinforced mortar laminates, Constr. Build. Mater. 23 (6) (2009) 2409–2420.
[4] F.A. Silva, R.D. Toledo Filho, J.A. Melo Filho, E.M.R. Fairbairn, Physical and mechanical properties of durable sisal fiber–cement composites, Constr. Build. Mater. 24 (5) (2010) 777–785.
[5] J.A. Melo Filho, F.A. Silva, R.D. Toledo Filho, Degradation kinetics and aging mechanisms on sisal fiber cement composite systems, Cem. Concr. Compos. 40 (2013) 30–39.
[6] R.D. Toledo Filho, K. Ghavami, G.L. England, K. Scrivener, Development of vegetable fiber–mortar composites of improved durability, Cem. Concr. Compos. 25 (2) (2003) 185–196.
[7] J. Claramunt, M. Ardanuy, J.A. García-Hortal, R.D. Toledo Filho, The hornification of vegetable fibers to improve the durability of cement mortar composites, Cem. Concr. Compos. 33 (5) (2011) 586–595.
[8] H. Savastano Jr., V.M. John, V. Agopyan, O.P. Ferreira, Weathering of vegetable fibre-clinker free cement composites, Mater. Struct. 35 (1) (2002) 64–68.
[9] G.H.D. Tonoli, S.F. Santos, H. Savastano Jr., S. Delvasto, R.M. Gutiérrez, M.M.L. Murphy, Effects of natural weathering on microstructure and mineral composition of cementitious roofing tiles reinforced with fique fibre, Cem. Concr. Compos. 33 (2) (2011) 225–232.
[10] J. Wei, C. Meyer, Utilization of rice husk ash in green natural fiber-reinforced cement composites: mitigating degradation of sisal fiber, Cem. Concr. Res. 81 (2016) 94–111.
[11] J. Wei, C. Meyer, Degradation mechanisms of natural fiber in the matrix of cement composites, Cem. Concr. Res. 73 (2015) 1–16.
[12] J. Wei, C. Meyer, Degradation rate of natural fiber in cement composites exposed to various accelerated aging environment conditions, Corros. Sci. 88 (2014) 118–132.
[13] J. Wei, C. Meyer, Improving degradation resistance of sisal fiber in concrete through fiber surface treatment, Appl. Surf. Sci. 289 (15) (2014) 511–523.
[14] B.J. Mohr, J.J. Biernacki, K.E. Kurtis, Supplementary cementitious materials for mitigating degradation of kraft pulp fiber-cement composites, Cem. Concr. Res. 37 (11) (2007) 1531–1543.
[15] B.J. Mohr, J.J. Biernacki, K.E. Kurtis, Microstructural and chemical changes in pulp fiber cement composites during wet/dry cycling, Cem. Concr. Res. 36 (7) (2006) 1240–1251.
[16] M. Ramli, W.H. Kwan, N.F. Abas, Strength and durability of coconut-fiber-reinforced concrete in aggressive environments, Constr. Build. Mater. 38 (2013) 554–566.
[17] C.S. Rodrigues, K. Ghavami, P. Stroeven, Rice husk ash as a supplementary raw material for the production of cellulose–cement composites with improved performance, Waste Biomass Valor 1 (2010) 241–249.
[18] M. Ardanuy, J. Claramunt, R.D. Toledo Filho, Cellulosic fiber reinforced cement-based composites: a review of recent research, Constr. Build. Mater. 79 (2015) 115–128.
[19] V. Agopyan, J.R.H. Savastano, V.M. John, M.A. Cincotto, Developments on vegetable fiber–cement cased materials in São Paulo, Brazil: an overview, Cem. Concr. Compos. 27 (5) (2005) 527–536.
[20] H. Savastano Jr., S.F. Santos, M. Radonjic, W.O. Soboyejo, Fracture and fatigue of natural fiber-reinforced cementitious composites, Cem. Concr. Compos. 31 (4) (2009) 232–243.
[21] M.F. Rosa, B. Chiou, E.S. Medeiros, D.F. Wood, T.G. Williams, L.H.C. Mattoso, W.J. Orts, S.H. Imama, Effect of fiber treatment on tensile and thermal properties of starch/ethylene vinyl copolymers/coir biocomposites, Bioresour. Technol. 100 (2009) 5196–5202.
[22] P. Saha, S. Manna, S.R. Chowdhury, R. Sen, D. Roy, B. Adhikari, Enhancement of tensile strength of lignocellulosic jute fbers by alkali-steam treatment, Bioresour. Technol. 101 (2010) 3182–3187.
[23] D. Ray, B.K. Sarkar, Characterization of alkali-treated jute fibers for physical and mechanical properties, J. Appl. Polym. Sci. 80 (2001) 1013–1020.
[24] C. Scheffler, S.L. Gao, R. Plonka, E. Mäder, S. Hempel, M. Butler, V. Mechtcherine, Interphase modification of alkali-resistant glass fibers and carbon fibers for textile reinforced concrete I: fiber properties and durability, Compos. Sci. Technol. 69 (3–4) (2009) 531–538.
[25] E. Mäder, R. Plonka, M. Schiekel, R. Hempel, Coatings on alkali-resistant glass fibers for the improvement of concrete, J. Ind. Text. 33 (3) (2004) 191–207.
[26] S.R. Ferreira, F.A. Silva, P.R.L. Lima, R.D. Toledo Filho, Effect of fiber treatments on the sisal fiber properties and fiber–matrix bond in cement based systems, Constr. Build. Mater. 101 (30) (2015) 730–740.
[27] S.R. Ferreira, P.R.L. Lima, F.A. Silva, R.D. Toledo Filho, Effect of sisal fiber hornification on the adhesion with portland cement matrices, Rev. Matéria 17 (2) (2012) 1024–1034.
[28] W. Brameshuber, Textile Reinforced Concrete. State of the Art Report of Rilem Technical Committee 201-TRC: Textile Reinforced Concrete, Rilem Publications, 2006. S.A.R.L.
[29] S.W. Mumenya, R.B. Tait, M.G. Alexander, Mechanical behaviour of textile concrete under accelerated ageing conditions, Cem. Concr. Compos. 32 (8) (2010) 580–588.
[30] M. Butler, V. Mechtcherine, S. Hempel, Experimental investigations on the durability of fiber–matrix interfaces in textile-reinforced concrete, Cem. Concr. Compos. 31 (4) (2009) 221–231.
[31] M. Butler, V. Mechtcherine, S. Hempel, Durability of textile-reinforced concrete made with AR glass fibre - effect of the matrix composition, Mater.

Struct. 43 (2010) 1351–1368.
[32] M. Butler, S. Hempel, V. Mechtcherine, Modelling of ageing effects on crack-bridging behaviour of AR-glass multifilament yarns embedded in cement-based matrix, Cem. Concr. Res. 41 (2011) 403–411.
[33] A. Bentur, M.Y. Yardimci, R. Tirosh, Preservation of telescopic bonding upon aging of bundled glass filaments by treatments with nano-particles, Cem. Concr. Compos. 47 (2013) 69–77.
[34] R.S.P. Coutts, Fibre-matrix interface in air-cured wood-pulp fibre-cement composites, J. Mater. Sci. Lett. 6 (1987) 140–142.
[35] H. Savastano Jr., V. Agopyan, Transition zone studies of vegetable fibre-cement paste composites, Cem. Concr. Compos. 21 (1999) 49–57.
[36] F.A. Silva, J.A. Melo Filho, S.R. Ferreira, R.D. Toledo Filho, On the durability and interface mechanisms of natural FRC: a material for the sustainable construction industry, in: SP-299 Fiber Reinforced Concrete for Sustainable Structures, American Concrete Institute, 2015, pp. 1–14. ACI Special Publication, 2015.
[37] J. Claramunt, L.J. Fernández-Carrasco, H. Ventura, M. Ardanuy, Natural fiber nonwoven reinforced cement composites as sustainable materials for building envelopes, Constr. Build. Mater. 115 (2016) 230–239.
[38] S.-L. Gao, E. Mäder, R. Plonka, Nanocomposite coatings for healing surface defects of glass fibers and improving interfacial adhesion, Compos. Sci. Technol. 68 (14) (2008) 2892–2901.
[39] Brazilian Standard NBR 11578, Cimento Portland Composto, Associação Brasileira de Normas Técnicas (ABNT), 1991 ([in Portuguese]).
[40] J. Dweck, A.L.C. Cunha, C.A. Pinto, J.P. Gonçalves, P.M. Büchler, Thermogravimetry on calcined mass basis – hydrated cement phases and pozzolanic activity quantitative analysis, J. Therm. Anal. Calorim. 97 (2009) 85–89.
[41] J.A. Melo Filho, Chemical and Thermal Durability and Mechanical Behavior of High Performance Sisal Cement Based Composites, Doctoral thesis, Civil Engineering Department, COPPE/UFRJ, 2012 ([in Portuguese]).
[42] Z. Yang, X. Shi, A.T. Creighton, M.M. Peterson, Effect of styrene–butadiene rubber latex on the chloride permeability and microstructure of Portland cement mortar, Constr. Build. Mater. 23 (2009) 2283–2290.
[43] S. Chakraborty, S.P. Kundu, A. Roy, B. Adhikari, S.B. Majumder, Polymer modified jute fibre as reinforcing agent controlling the physical and mechanical characteristics of cement mortar, Constr. Build. Mater. 49 (2013) 214–222.